Analysis of cymbal vibrations using nonlinear signal processing methods

Cyril Touzé[1] , Antoine Chaigne[1], Thomas Rossing[2] and Staffan Schedin[3].

[1] *ENST, Signal and Image Processing Department, 46 rue Barrault 75634 Paris Cedex 13, France.*
[2] *Department of Physics, Northern Illinois University, DeKalb, IL 60115, USA.*
[3] *Division of Experimental Mechanics, Luleå University of Technology, SE-97187 Luleå, Sweden.*

Abstract: Cymbal vibrations are analyzed using general tools of nonlinear dynamics. The signals were obtained from experiments conducted on a thin crash cymbal excited by a shaker at its center. Due to the slowly-increasing amplitude of the shaker motion, transitions from linear to chaotic motion of the cymbal are observed. An analysis based, first, on Short-Time Fourier Transform and, secondly, on the reconstruction of the phase space trajectory, is carried out in order to characterize the successive transitions of the nonlinear regime which precedes the chaotic motion. One of the most salient observed feature in this part of the signal is the combination of resonances. Finally, the properties of the cymbal vibration, in its chaotic part, are characterized with the help of two different techniques: the method of false nearest neighbors and the correlation dimension. From the results of these two methods both a lower and an upper bound for the number of active degrees of freedom (i. e. the number of coordinates needed to model the dynamics of the system) are obtained.

1. INTRODUCTION

The dynamical behavior of nonlinear percussive instruments, such as cymbals and gongs, is not well understood. Previous work on cymbals has been mainly concerned with accurate and extensive measurements of eigenfrequencies and eigenmodes in the linear regime [1], [2], or with the musical effects such as the characteristic bright shimmering sound [3]. The observed frequency shifts and the energy transfer from the low to high frequency domain in gongs and tamtams have also been investigated [4], [5, chapter 20]. However, a detailed understanding of the complicated mechanisms involved in the generation of sound by these instruments remains challenging.

The principal aim of the work presented here is to take advantage of the existing tools in both the signal processing and chaos physics communities to extract as much as possible information from the analysis of cymbal vibrations and to characterize the dynamics of this mechanical system when driven continuously from its linear to chaotic behavior. Accurate measurements of eigenfrequencies previously made on the cymbal used for the experiments serve as references for a better understanding of the phenomena involved in the nonlinear regime [2].

The analysis of the chaotic vibrations of the cymbal yields an estimate of the number of *active degrees of freedom* which characterizes the system. As mentioned by Lauterborn et al., this notion of *active degree of freedom* should not be mistaken for its significance in a linear context where one degree of freedom is associated to each mode [6]. In chaos physics, this number refers to the number of state space coordinates which are necessary to model the system. It can be expected that the knowledge of the number of active degrees of freedom will be a guideline in the future for developing simple mechanical models presenting a similar behavior than the one observed in cymbals.

2. EXPERIMENTS

Previous experiments in which a cymbal was driven to chaos by means of a shaker [7], [8], have been reproduced by S. Schedin. The cymbal used is a Zildjian thin crash cymbal, of diameter 41 cm. It is clamped at its center to an impedance head (B&K8001) mounted to a vibration exciter (manufactured by LDS). The exciter is driven by a sinusoidal signal. The time response of the cymbal (acceleration at two points on the cymbal and sound pressure at two positions) is measured as the excitation amplitude is increased linearly and very slowly. To achieve a slow linear increase of the amplitude, the sinusoidal signal driving the exciter is modulated by a triangle wave of a very low frequency.

A small B&K accelerometer (No.4393, 2.4 g) is attached either at the edge or at half the radius of the cymbal. The sound pressure is recorded using a microphone (B&K4165), positioned either in the near-field to the cymbal (a few centimeters from its edge) or in the far-field (about 1 m from the cymbal). The eigenfrequencies have been slightly readjusted in order to account for both the accelerometer's mass and the clamped condition at the center. Measurements are performed for a number of selected driving frequencies. Thus, for each driving frequency, four recordings are conducted. A two-channel DAT recorder was used to register the excitation signal (from the impedance head) and the response signal (either from the accelerometer or the microphone). All the measurements were conducted in an anechoic room.

It has been observed that, for a given driving frequency and a given value of the amplitude of the shaker, the acceleration spectra at the two different positions, do not exhibit the same frequency content. In addition, from the comparison between frequency analysis of sound pressure and acceleration signals, it turns out that the power spectra again exhibit a significantly different content. One possible explanation for these spectral observations may be that the bifurcations imply local phenomena and that the emitted sound spectra, on the contrary, give a global picture of the nonlinear motion. Therefore, in this study, we limit ourselves with the analysis of the acceleration signals.

3. SHORT TIME FOURIER TRANSFORM AND TIME SERIES ANALYSIS

This section is concerned with the analysis of the quasi-linear part of the cymbal acceleration, i.e. before the chaotic regime is established. The length of this part of the time series is nearly equal to 10 s. In this part, the amplitude of the signal increases slowly so it can be considered as quasi-stationary over about 1 s. A "Short-Time" Fourier Transform with a Blackman-Harris window is conducted on successive portions of the signal of length 0.68 s (32768 samples at 48 kHz) and a zero-padding with a factor of 2 is applied. As a consequence, the spectral peaks are measured with 0.73 Hz accuracy.

The nonlinear time series analysis of the signal is based on the reconstruction of the phase space trajectory, which provides a topological equivalent representation of the real phase space of the system. The method is based on the theorem by Takens and Mañe (see [9], [6]). The phase space representation yields a good understanding of the bifurcations and allows the calculation of the invariants of the motion which are not available from the spectra, as it will be done in the next section.

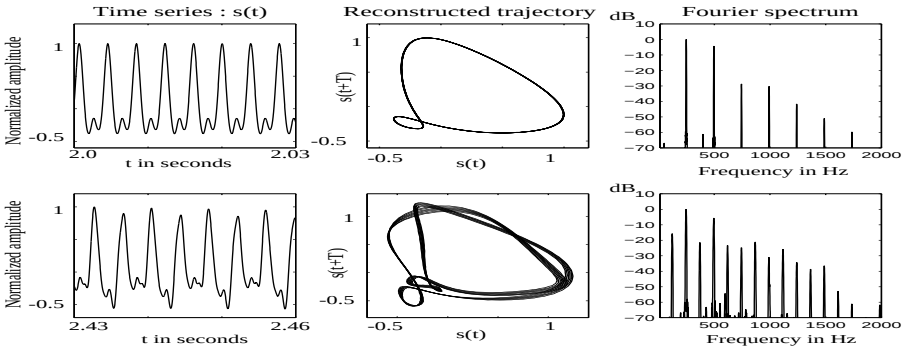

Figure 1: Time series, phase space trajectory and Fourier spectrum at two different instants of time for the acceleration recorded at the edge of the cymbal with driving frequency $F_{exc} = 248Hz$.

From the observation of the time series $s(n)$ measured by the accelerometer, where $n = 1...N$ is the time index, a multivariate trajectory is constructed with:

$$y(n) = [s(n), s(n+T), ..., s(n+(d_E-1)T)], \quad n = 1, ..., N-(d_E-1)T. \tag{1}$$

where T is the time delay and d_E the so-called *embedding dimension.* The best choice for the values of T and d_E is a question which has been largely investigated [10]. A widely used method has been selected here where T is the first minimum of the so-called *average mutual information function* [11]. The choice of d_E is based on the false nearest neighbors method presented in the following section.

Figure 1 and 2 illustrate two typical cases. Each figure shows in successive columns: the temporal shape of the acceleration time series (in normalized units), the trajectory in the phase space reconstructed with the time delay method described before and with d_E=2, and the Fourier spectrum. The amplitude of the shaker increases in each row from the top to the bottom of the figures. For the sake of clarity, only a short portion of the acceleration signal and only the low-frequency part of the spectra are displayed.
Figure 1 corresponds to the case where the driving frequency ($F_{exc} = 248Hz$) is twice as much as the eigenfrequency (124 Hz) corresponding to the eigenmode (4,0). One can see a clear period doubling.

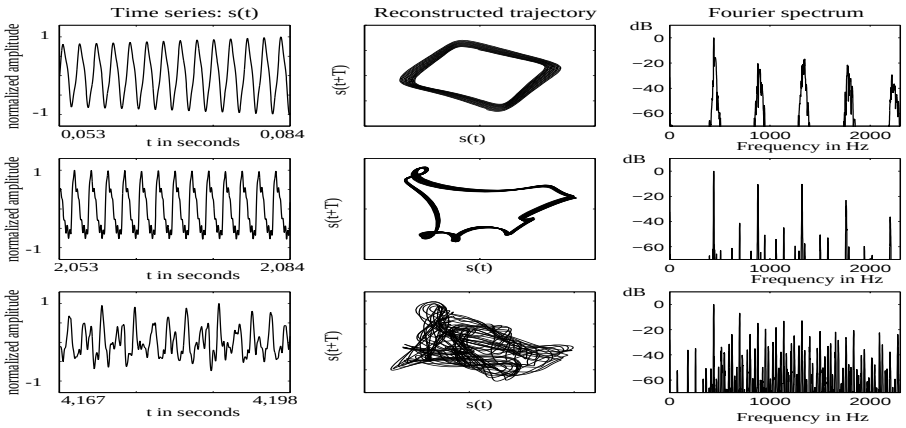

Figure 2: Acceleration signal recorded at about half a radius away from the edge of the cymbal, with $F_{exc} = 440Hz$. With increasing amplitude of the excitation, the ratio between the frequencies of the spectral peaks and the driving frequency is not integral. Typical foldings of the trajectory can be seen in the phase space. The last row (bottom) corresponds to the beginning of the chaotic regime.

Another typical result is obtained when the driving frequency is not harmonically related to one particular eigenfrequency of the cymbal. Figure 2 illustrates this case for $F_{exc} = 440\ Hz$. In this case, spectral peaks are displayed at frequencies whose ratios with the driving frequency are not integral. This shows that the phenomena involved are not a simple generation of subharmonics of the excitation frequency. Moreover, the phase space trajectory shows some foldings which are typical of the Ruelle-Takens *route to chaos*, i.e. appearance of frequencies that are incommensurate (whose ratio is not a rational number) and transition from quasiperiodicity to chaos, see [12] for more details. A closer analysis of the spectral peaks, which consists in investigating the relations between the most salient frequencies in the spectra, has been made. It is found that the spectral peaks are linked by relations of the form $F_{exc} = f_\alpha \pm f_\beta$, where f_α and f_β are eigenfrequencies of the system. Figure 2, for example, shows spectral peaks at 77 Hz, 182 Hz, 259 Hz and 363 Hz in the interval [0, 440 Hz], and the following relations are obtained:

$$182 + 259 = 441 \simeq F_{exc} \quad ; \qquad 77 + 363 = 440 = F_{exc} \tag{2}$$

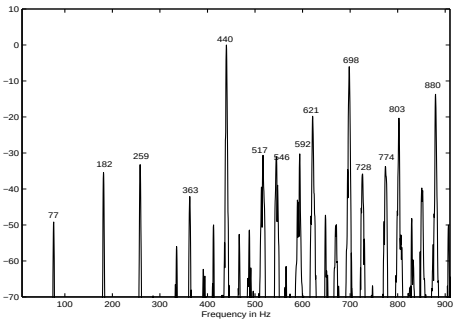

Figure 3: Combination peaks for the driving frequency : $F_{exc} = 440$ Hz (Enlargement of the last spectrum in figure 2).

Noticing that for the cymbal clamped at its center and with the accelerometer glued at r/2, the (3,0) mode is at 75,5 Hz, the (5,0) mode at 177 Hz, the (6,0) mode at 234,5 Hz and the (8,0) mode at 359,5 Hz. one can observe a set of resonances which combine a few number of eigenfrequencies. This property, which is characteristic of systems with quadratic nonlinearity [13], has been observed for each driving frequency having no particular harmonic relationship with one eigenfrequency of the cymbal. This incite us to describe the observed bifurcations in terms of excited modes, and not only in terms of subharmonics. In other words, the common observed feature is not the generation of subharmonics, but the appearance of frequencies such that their sum, or their difference, is equal to the driving frequency.

The different transitions can be grouped into one unique scenario, since the period doubling has only been observed in the particular case where the driving frequency was equal to twice one particular eigenfrequency. Thus, a period doubling can be seen as a particular case of the general described combinations, where $F_{exc} = 2f_\alpha$.

In each experiments conducted with the cymbal, only one or two transitions were observed before the chaos. This is in agreement with previous experiments [8]. It is a general feature of systems exhibiting very little dissipation (or Hamiltonian systems). Another property of such systems is that the phase space trajectory does not show a clear attractor with a fractal structure, as it is observed in very dissipative system [14]. This explains the last row of figure 2 that display a blurred structure.

4. ESTIMATING THE NUMBER OF ACTIVE DEGREES OF FREEDOM

The essential purpose of the analysis performed in the chaotic regime of the cymbal acceleration was to bound the number of active degrees of freedom by using two differents techniques: the method of *false nearest neighbors* and the *correlation dimension.*

The method of *false nearest neighbors* is presented in [15], [10]. The basic idea is to determine the embedding dimension d_E of the system for which the attractor is unfolded. This dimension is obtained when all points which are close in the reconstructed phase space are neighbors because of the dynamics of the system and not because of the projection of the state space trajectory onto a too small embedding space. In this latter case, the close points are said *false neighbors.*

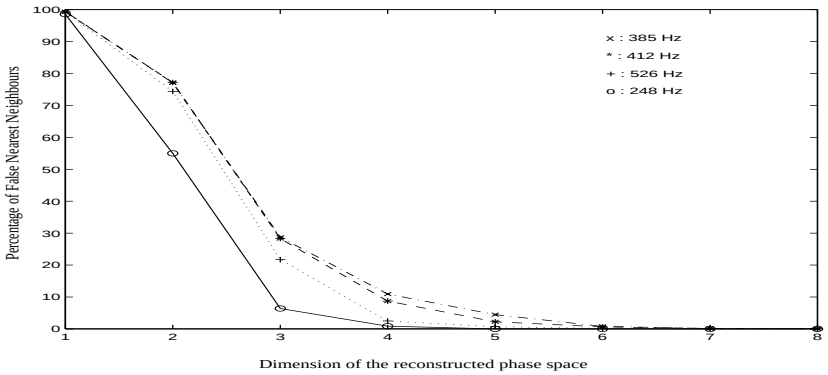

Figure 4: Percentage of false nearest neighbors as a function of the dimension of the phase space for 4 different driving frequencies. The acceleration is recorded at the edge of the cymbal for each driving frequency, except for 248 Hz for which the signal is recorded at half a radius from the edge.

The determination of the embedding dimension d_E with this method yields an upper bound for the value of the number m of active degrees of freedom:

$$m \leq d_E \tag{3}$$

since we cannot have more degrees of freedom than the number of coordinates. The algorithm proceeds as follows [15]:

- In d-dimension phase space, for each vector $y(n) = [s(n), s(n+T), ..., s(n+(d-1)T)]$ of the reconstructed attractor, the nearest neighbor $y'(n)$ is selected.
- In dimension d+1, it is checked if $y(n)$ and $y'(n)$ are still neighbors or not.
- As the dimension d increases, the percentage of false nearest neighbors is determined. When this percentage reaches the value zero, we can be confident in the fact that the attractor is unfolded, and we get the value $d = d_E$.

The results of this method, for 4 different driving frequencies, are shown in Fig. 4. This figure shows that a minimum embedding dimension can be found for each signal, i.e. that the attractor can be unfolded in phase space. It can be seen that the percentage of false nearest neighbors tends to zero when the dimension of the phase space is equal to 7. This value can be considered as an upper bound for the number m of degrees of freedom.

The *correlation dimension* d_2 of the signal has been determined in order to obtain a lower bound for m. Its determination is based on the calculation of the correlation integral (see [16], [17], [18]).

The correlation dimension is related to the number m of degrees of freedom by the inequalities:

$$[d_2] \leq m \leq [2d_2 + 1] \tag{4}$$

where the brackets [] indicate rounding to the next greater integer. The lower bound simply expresses the fact that the dimension of the phase space cannot be less than d_2 and the upper bound is a consequence of the reconstruction theorem of Takens and Mañé which will not be demonstrated here [9].

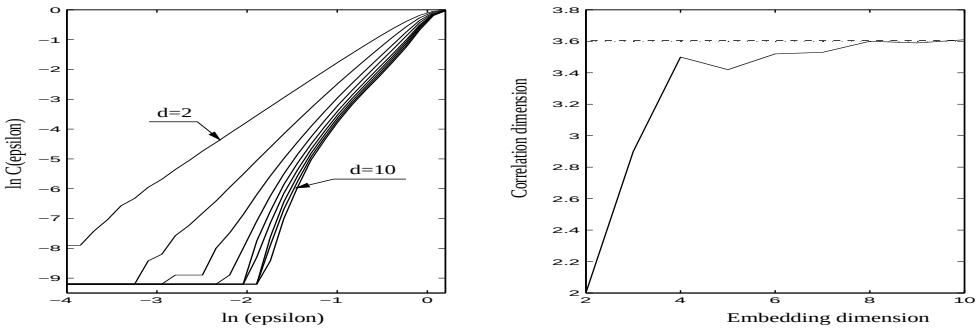

Figure 5: (left) Correlation integral C(ε)for the signal recorded at the edge of the cymbal, with $F_{exc} = 526Hz$, for embedding dimensions running from 2 to 10. (right) Values of the correlation dimension (slope of the correlation integral) as a function of the embedding dimension. In this case, it is found that the correlation dimension d_2 tends asymptotically to 3.6.

In practice, the correlation dimension is obtained by measuring the spatial correlations between points in the reconstructed phase space, which is done by counting the number of points whose mutual distance is less than a given value ε. For a given embedding dimension d_E, the correlation integral is calculated from the multivariate phase space representation (equation(1)):

$$C(\varepsilon) = \frac{1}{N(N-1)} \sum_{i \neq j} H(\varepsilon - ||y(i) - y(j)||) \tag{5}$$

where H is the Heaviside function, N the number of points and $||.||$ the infinite norm on $\mathbb{R}^{d_E}$. Grassberger and Procaccia show in [16] that the correlation integral behaves like: $C(\varepsilon) \sim \varepsilon^{d_2}$. To get the value of d_2, one has then to plot the curve $\ln C(\varepsilon)$ versus $\ln \varepsilon$ in order to extract the slope.

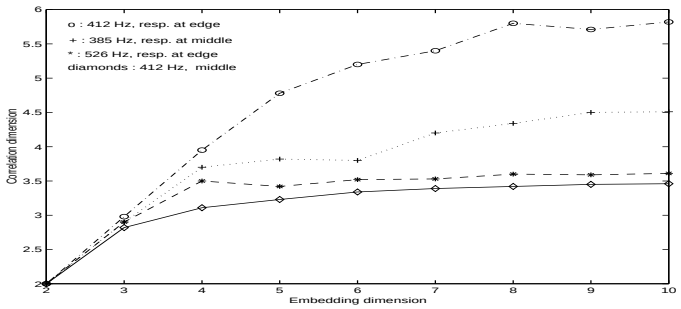

Figure 6: Correlation dimension vs. embedding dimension for 4 different excitation frequencies. The correlation dimension d_2 is given by the asymptotic limit of the curves as the embedding dimension increases.

The algorithm proceeds as follows: for increasing values of the embedding dimension, the correlation integral is calculated and the slope of the curve is extracted. For deterministic systems, the slope converges to a finite value which is defined as the correlation dimension d_2 whereas the slope would tend to infinity for a random noise (see Fig. 5).

Figure 6 shows typical results for the cymbal, for 4 different driving frequencies and with 40000 samples. In each case, the correlation dimension tends to a limit as the embedding dimension increases which proves that the dynamics of the system can be reduced to a low-dimensional deterministic process. The complete results of the correlation dimension calculations are shown in Table 1.

Driving Frequency	**385 Hz**	**385 Hz**	**526 Hz**	**412 Hz**	**412 Hz**	**248 Hz**	**440 Hz**
Accelerometer position	**r/2**	**edge**	**edge**	**r/2**	**edge**	**r/2**	**r/2**
Correlation dimension: d_2	4,5	4,6	3,6	3,4	5,8	2,7	3,8
Embedding dimension: d_E	6	7	5	5	6	5	5

Table 1: Estimation of the number of active degrees of freedom. For each driving frequency, the calculation of the correlation dimension with 40000 points and the minimum embedding dimension given by the false nearest neighbors method with 10000 points are presented. The values obtained for each frequency are of the same order of magnitude.

5. CONCLUSION

Nonlinear signal processing tools yield bounds for the number of active degrees of freedom. This must be understood as a first step in the modeling of the cymbal. Once the number m of active degrees of freedom has been estimated, one knows that a model of the system will be composed of m equations. The results, summarized in Table 1, show, according to equations (3) and (4), that m can be bounded as follows:

$$3 \leq m \leq 7$$

The upper bound is the maximum value of d_E found for the different signals and the lower bound is the minimum value given by the correlation dimension d_2. This shows that we have a low-dimensional deterministic process that can be modeled with m equations.
The analysis conducted in section 3 shows that only a few number of eigenmodes are involved in the nonlinear dynamics and that typical combinations of these modes are obtained for each driving frequency. These results should be of help for developing a low-dimensional model for the dynamics of the cymbal.

ACKNOWLEDGEMENTS

We are grateful to the authors of [11] for providing us with their public domain C programs to calculate the averaged mutual information function, and to Paul Manneville for fruitful discussions.

REFERENCES

1. T.D. Rossing and R.W. Peterson. *Percussive Notes*, 19(3):31–41, 1982.
2. C. Wilbur and T.D. Rossing. ASVA, Tokyo, 1997.
3. T.D. Rossing and R.B. Sheperd. In *Proc. 11th Intl. Congress on Acoustics (Paris)*, pages 329–333, 1983.
4. K.A. Legge and N.H. Fletcher. *J. Acoust. Soc. Am.*, 86(6):2439–2443, 1989.
5. N.H. Fletcher and T.D. Rossing. *The physics of musical instruments.* Springer-Verlag, New-York, 1991.
6. W. Lauterborn and U. Parlitz. *J. Acoust. Soc. Am.*, 84(6):1975–1993, 1988.
7. N.H. Fletcher. In D. Green and T. Bossomaier, editors, *Complex systems: from Biology to computation.* IOS, Amsterdam, 1993.
8. C. Wilbur and T.D. Rossing. *J. Acoust. Soc. Am.*, 101(5):3144, 1997. Pt.2.
9. F. Takens. In *Lecture notes in Mathematics*, volume 898, pages 366–381. Springer-Verlag, Berlin, 1981.
10. H.D.I Abarbanel. *Analysis of observed chaotic data.* Springer-Verlag, New-York, 1996.
11. A.M. Fraser and H.L. Swinney. *Physical Review A*, 33(2):1134–1140, 1986.
12. H.G. Schuster. *Deterministic chaos.* VCH, Weinheim, third augmented edition, 1995.
13. A.H. Nayfeh and D.T. Mook. *Nonlinear oscillations.* John Wiley, New-York, 1979.
14. F.C. Moon. *Chaotic vibrations.* John Wiley & sons, New-York, 1987.
15. M.B. Kennel, R. Brown, and H.D.I. Abarbanel. *Physical Review A*, 45(6):3403–3411, 1992.
16. P. Grassberger and I. Procaccia. *Physica 9D*, pages 189–208, 1983.
17. P. Grassberger, T. Schreiber, and C. Schaffrath. *Int. J. of Bifurcation and Chaos*, 1(3):521–547, 1991.
18. J. Theiler. *J. Opt. Soc. Am.*, 7(6):1055–173, 1990.